Supplementary Material for

Characterization and Spatial Source Apportionments of Ambient PM_{10} and $PM_{2.5}$ during the Heating Period in Tian'jin, China

Baoshuang Liu[1], Xiaoyun Sun[1], Jiaying Zhang[1], Xiaohui Bi[1*], Yafei Li[1], Liwei Li[2], Haiyan Dong[2], Zhimei Xiao[2], Yufen Zhang[1], Yinchang Feng[1]

[1]*State Environmental Protection Key Laboratory of Urban Ambient Air Particulate Matter Pollution Prevention and Control & Center for Urban Transport Emission Research, College of Environmental Science and Engineering, Nankai University, Tian'jin 300350, China*

[2]*Tianjin Eco-Environment Monitoring Center, Tian'jin, 300071, China*

**Corresponding author.*
E-mail address: bixh@nankai.edu.cn (X. Bi). Nankai University, No.38 Tongyan Road, Jinnan District, Tian'jin, P.R. China 300350

2.2 Ambient sampling

Polypropylene and quartz fibre filters were baked in the oven at 60°C and 400–500°C before sampling. All filters were kept equilibrated at least three days under a stable environment with a temperature and relative humidity of 22°C and 45–55% before and after sampling. All filters were stored at –4°C before chemical analysis. For gravimetric analysis, all filter membranes were weighted twice on a microbalance with resolution of 0.01 mg (Mettler Toledo, AX205) before and after sampling. An electrostatic eliminating device was used to ensure the accuracy of gravimetric results.

2.3 Chemical analysis

For elements analysis, one eighth of polypropylene filters was cut into fragments and placed into an acid digestion tank before determining. The acid solutions (4 mL nitric acid, 2 mL hydrochloric acid and 1 mL hydrogen peroxide) were put into the tank, and then tank was digested by microwave oven. The solution was decanted into a test tube and diluted to 25 mL with deionized water after being cooled and filtered. For quality assurance and quality control (QA/QC), pretreated standard reference materials were analyzed with the same procedure, ensuring that the recovered values for all of the target elements falling into the range or within 5% of certified values.

For water-soluble ions analysis, one eighth of each quartz fiber filter was placed into a glass tube, and deionized water was used to extract. The extraction procedure was carried out for at least three times, so that the water-soluble ions in particulate samples were extracted completely into the solution. Standard solutions of ions were prepared and detected for more than three replicates, and low relative standard deviations were observed.

For OC and EC analysis, further details of determining process are given in Liu et al. (2018). The analyzer was calibrated each day before and after the OC and EC analyses, and the first sample was analyzed again for every ten samples to ensure analysis precision. Additionally, the blank and duplicate samples analysis were conducted in order to ensure QA/QC (Liu et al., 2016a; Xue et al., 2010).

2.4 PMF and error estimation model

The principle for PMF model can be described by:

$$X_{ij} = \sum_{k=1}^{p} g_{ik} f_{kj} + e_{ij} \quad (1)$$

PMF is used to identify a number of factor (*p*), the species profile (*f*) of each source, and the contribution (*g*) of each factor (see Eq. (1) above, where e_{ij} is the residual for each sample).

To evaluate the stability of the solution, the object function *Q* was used to review the distribution of each species. The aim of PMF is to minimize the object function *Q* to reduce uncertainty (*u*)**:**

$$Q = \sum_{i=1}^{n} \sum_{j=1}^{m} \left[\frac{x_{ij} - \sum_{k=1}^{p} g_{ik} f_{kj}}{\mu_{ij}} \right]^2 \quad \textbf{(2)}$$

where μ_{ij} represents the uncertainty of *j*th species in the *i*th sample, which is used to weight the observations that include the missing data, sampling errors and detection limits (Paatero, 2007).

Before modeling, missing values are replaced by the mean of each species, with an uncertainty of four times the median. Values below method detection limits (MDLs) are retained and the uncertainties are set at 5/6 of detection limit values (Brown et al., 2015). Uncertainty of value greater than the MDL is defined as Eq. (3). And error fraction was suggested as 10% by Paatero (2000).

$$\text{Uncertainty} = \sqrt{(Error\ Fraction \times concentration)^2 + (0.5 \times MDL)^2} \quad \textbf{(3)}$$

2.5 Backward trajectory and PSCF model

The PSCF value for the *ij*th cell is expressed as:

$$PSCF_{ij} = \frac{m_{ij}}{n_{ij}} \quad \textbf{(4)}$$

where *i* and *j* is latitude and longitude, n_{ij} represents the total number of endpoints that fall in the grid cell, and m_{ij} is on behalf of the number of endpoints for the same cell corresponding to samples that are more than the threshold criterion.

The guideline values (24 h) of Ministry of Environmental Protection of China 2012 $PM_{2.5}$ and PM_{10} (75 μg m^{-3}, 150 μg m^{-3}, respectively) were taken as the criterion-values during the studying period. To reduce the effect of low values of n_{ij}, a weighting function W(n_{ij}) was multiplied into PSCF value to better reflect the uncertainty in cells (Dimitriou et al., 2015; Polissar et al., 2001). The weight function is described by:

$$WPSCF_{ij} = \frac{m_{ij}}{n_{ij}} * W(n_{ij}) \quad \textbf{(5)}$$

$$W(n_{ij}) = \begin{cases} 1.00, 3n_{ave} < n_{ij} \\ 0.70, 1.5n_{ave} < n_{ij} \leqslant 3n_{ave} \\ 0.40, n_{ave} < n_{ij} \leqslant 1.5n_{ave} \\ 0.20, n_{ij} < n_{ave} \end{cases} \quad \textbf{(6)}$$

Reference

Brown, S.G., Eberly, S., Paatero, P. and Norris, G.A. (2015). Methods for estimating uncertainty in PMF solutions: Examples with ambient air and water quality data and guidance on reporting PMF results. *Sci. Total Environ.* 518–519: 626–635.

Dimitriou, K., Remoundaki, E., Mantas, E. and Kassomenos, P. (2015). Spatial distribution of source areas of $PM_{2.5}$ by Concentration Weighted Trajectory (CWT) model applied in $PM_{2.5}$ concentration and composition data. *Atmos. Environ.* 116: 138–145.

Liu, B.S., Cheng, Y., Zhou, M., Liang, D.N., Dai, Q.L., Wang, L., Jin, W., Zhang, L.Z., Ren, Y.B., Zhou, J.B., Dai, C.L., Xu, J., Wang, J., Feng, Y.C. and Zhang, Y.F. (2018). Effectiveness evaluation of temporary emission control action in 2016 in winter in Shijiazhuang, China. *Atmos. Chem. Phys.* 18: 7019–7039.

Liu, B.S., Song, Na., Dai, Q.L., Mei, R.B., Sui, B.H., Bi, X.H. and Feng. Y.C. (2016a). Chemical composition and source apportionment of ambient $PM_{2.5}$ during the non-heating period in Taian, China. *Atmos. Res.* 170: 23–33.

Paatero, P. (2007). User's Guide for positive Matrix Factorization programs PMF2 and PMF3, part 1 e 2: Tutorial, 19–21. University of Helsinki, Helsinki, Finland.

Paatero, P. (2000). User's Guide for Positive Matrix Factorization Programs PMF2 andPMF3, Part 1: Tutorial. University of Helsinki, Finland (February).

Polissar, A.V., Hopke, P.K. and Harris, J.M. (2001). Source regions for atmospheric aerosol measured at Barrow, Alaska. *Environ. Sci. Technol.* 35: 4214–4226.

Xue, Y.H., Wu, J.H., Feng, Y.C., Dai, L., Bi, X.H. and Li, X. (2010). Source characterization and apportionment of PM_{10} in Panzhi-hua, China. *Aerosol Air Qual. Res.* 10: 367–377.

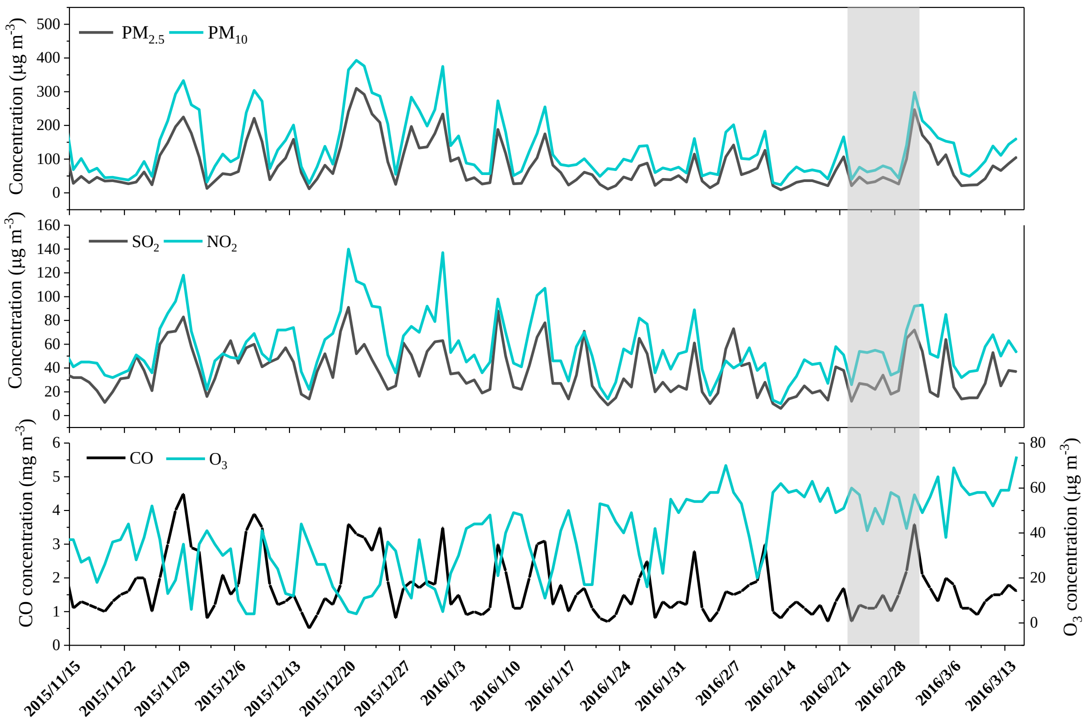

Fig. S1 Time series of air pollutants in Tian'jin during the heating period (from November 15th 2015 to March 15th 2016). The grey shadows represent the sampling period in this study.

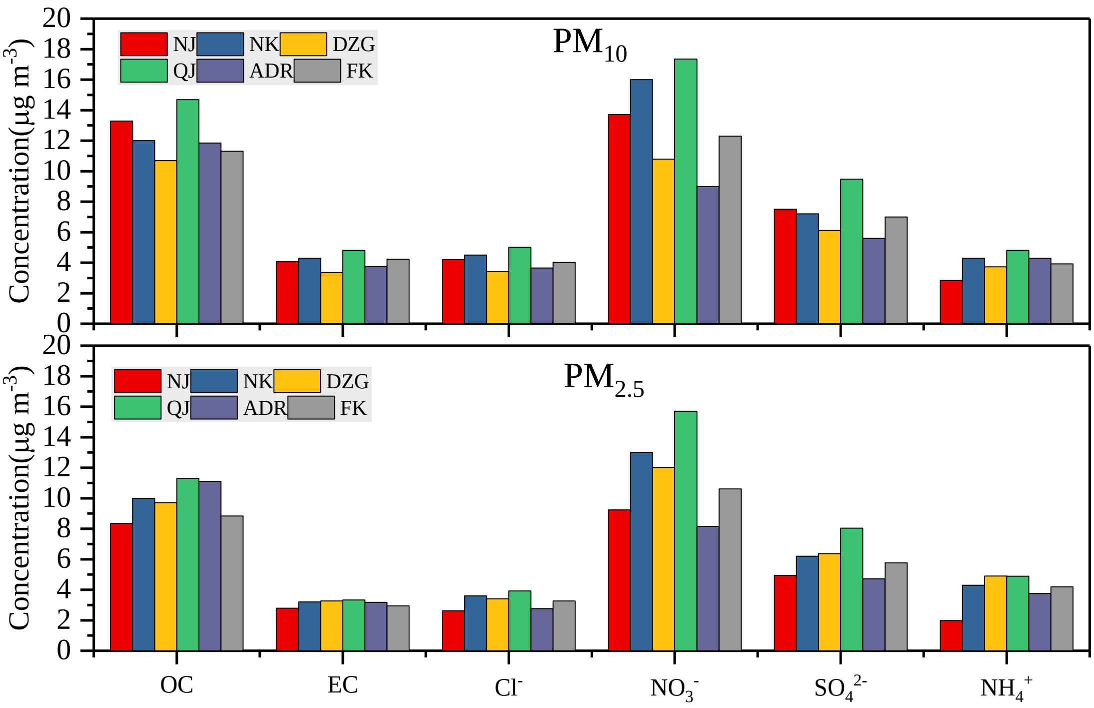

Fig. S2 The concentrations of the predominant water soluble ions in PM_{10} and $PM_{2.5}$ at different sampling sites. NJ: Nanjing Road, NK: Nankou Road, DZG: Dazhigu Road, ADR: Advancing Road, QJ: Qinjian Road, FK: Fukang Road.

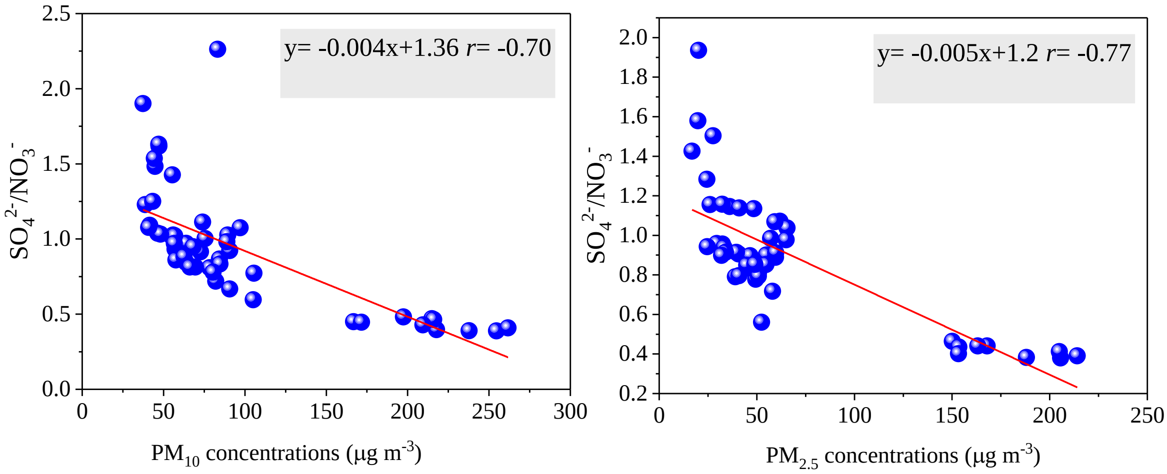

Fig. S3 Correlations between PM_{10} and $PM_{2.5}$ concentrations and SO_4^{2-}/NO_3^- during the heating period in Tian'jin.

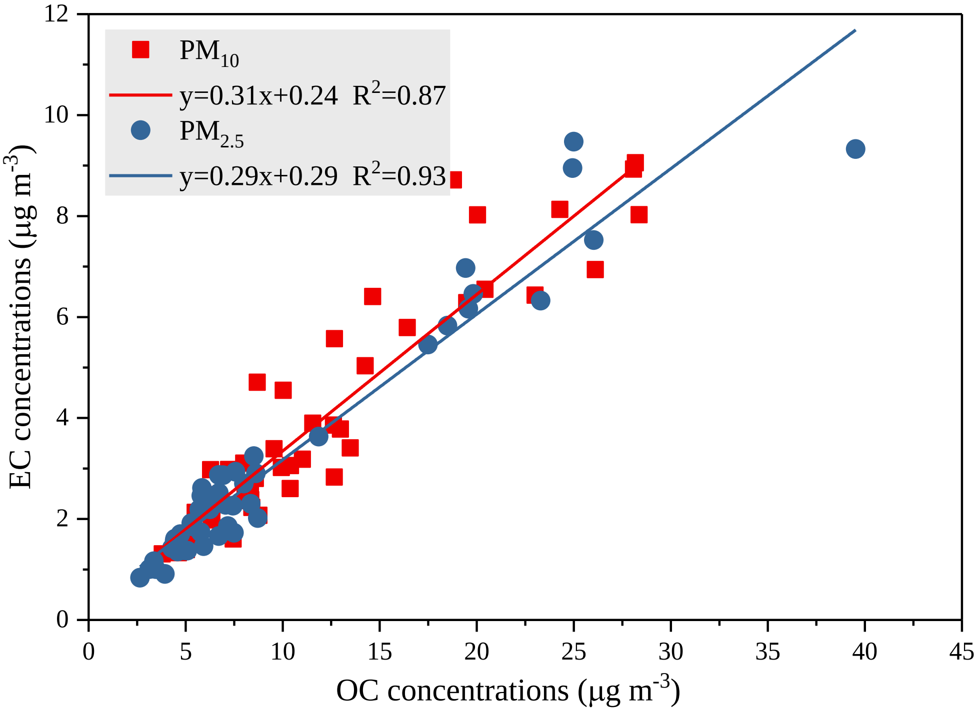

Fig. S4 Correlations between OC and EC in PM_{10} and $PM_{2.5}$ during the heating period at Tian'jin.

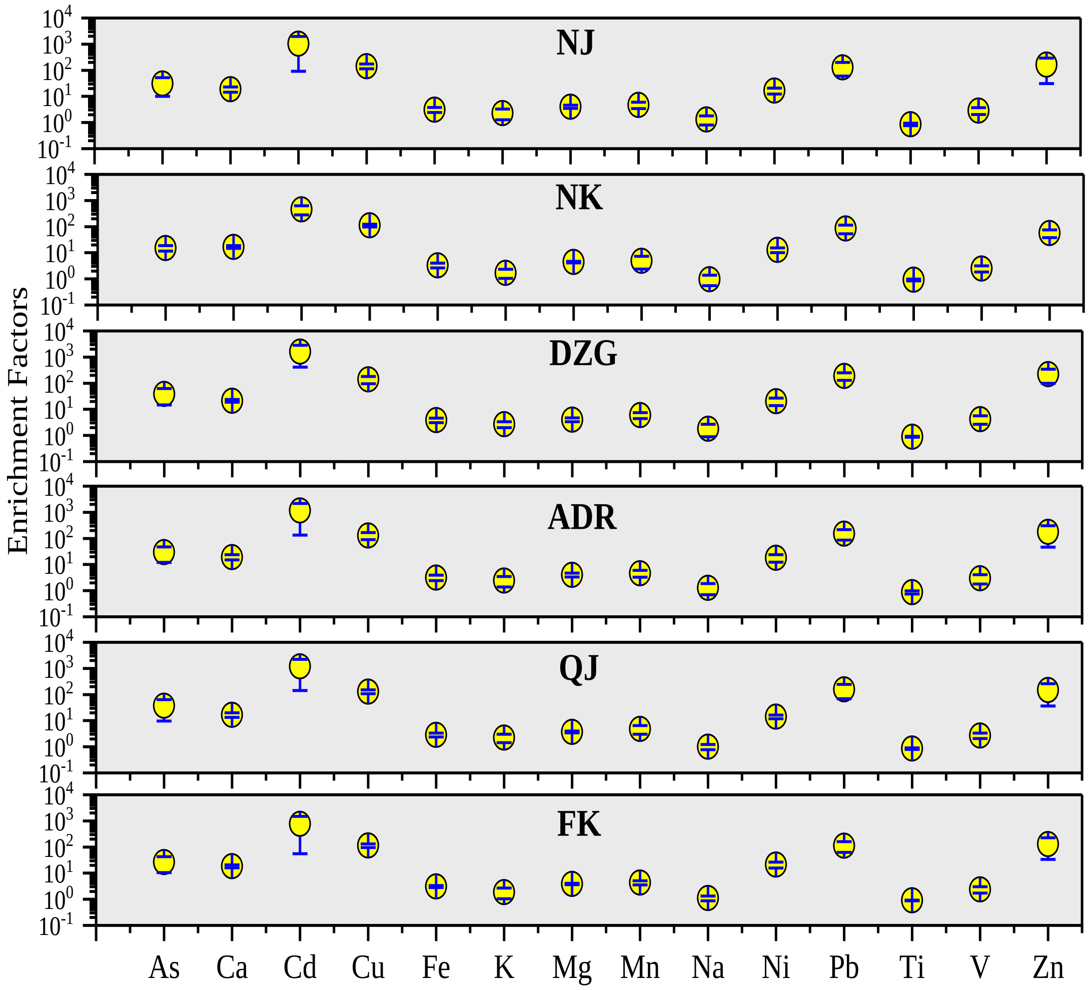

Fig. S5 Enrichment factors of trace elements in PM_{10} at different sampling sites. NJ: Nanjing Road, NK: Nankou Road, DZG: Dazhigu Road, ADR: Advancing Road, QJ: Qinjian Road, FK: Fukang Road.

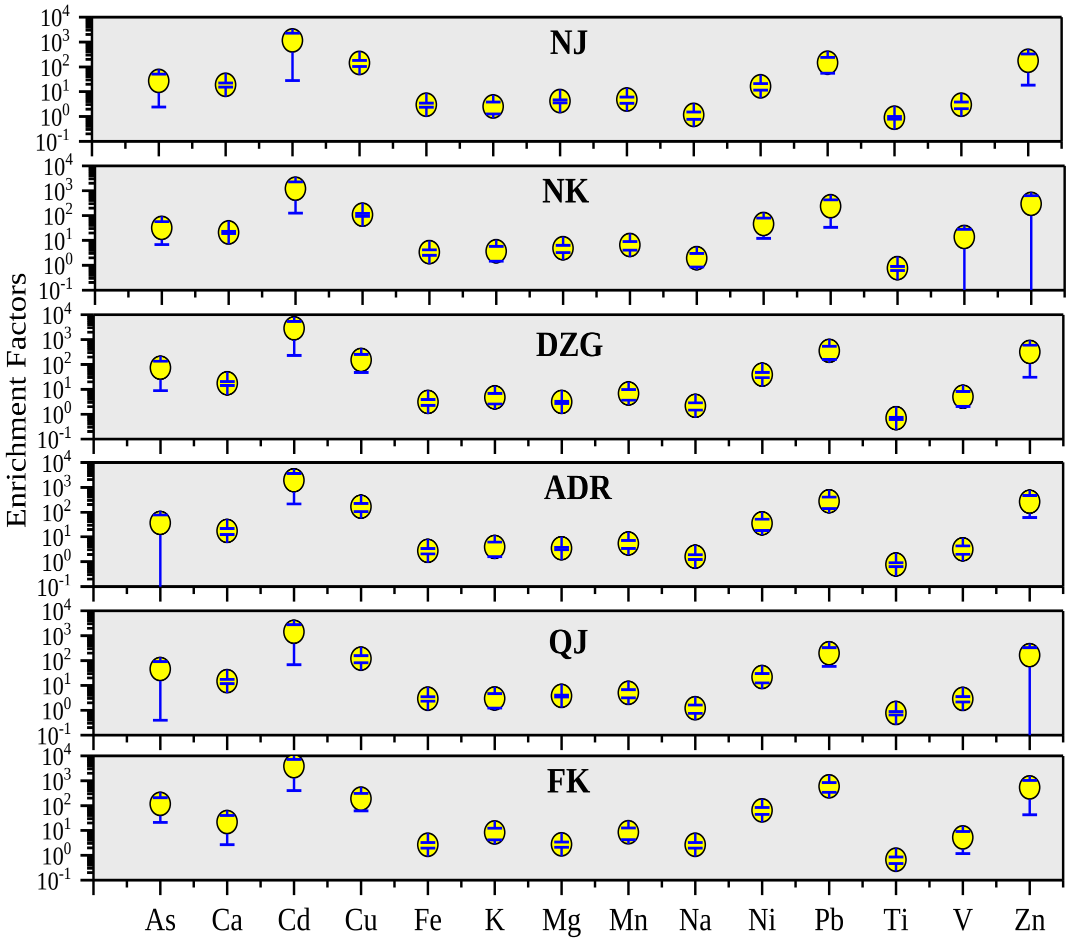

Fig. S6 Enrichment factors of trace elements in $PM_{2.5}$ at different sampling sites. NJ: Nanjing Road, NK: Nankou Road, DZG: Dazhigu Road, ADR: Advancing Road, QJ: Qinjian Road, FK: Fukang Road.

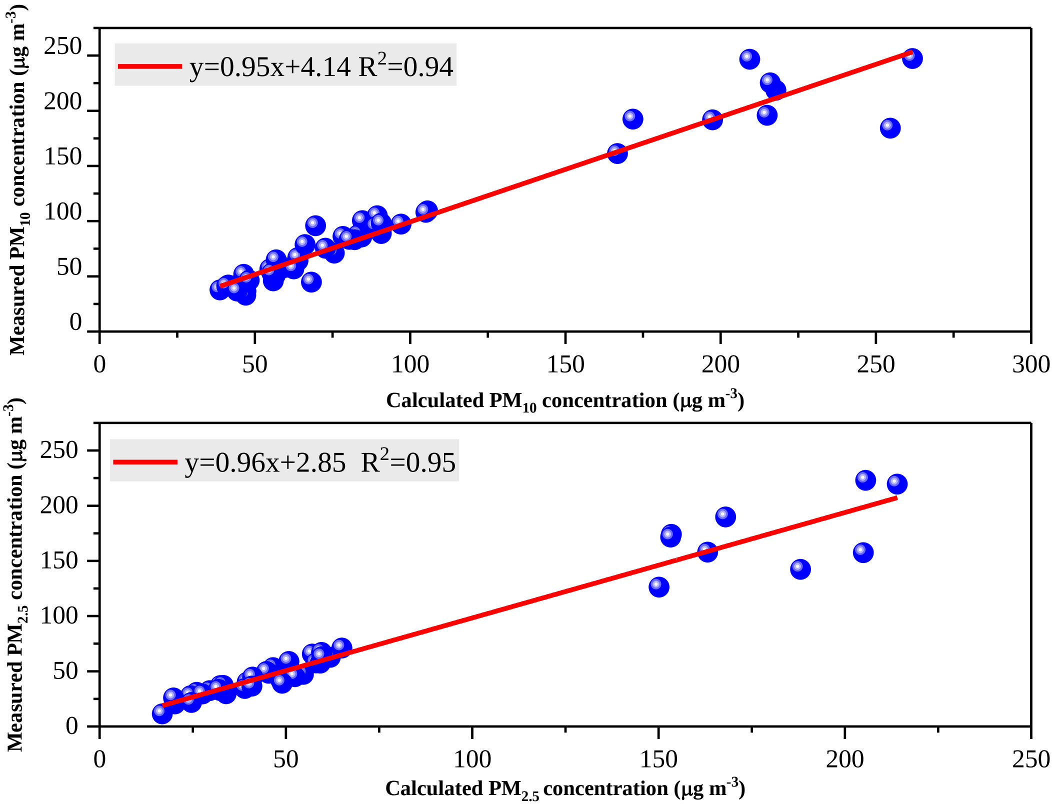

Fig. S7 Correlations between calculated and measured PM concentrations during heating season in Tian'jin. Also shown are the linear regression lines with regression equations.

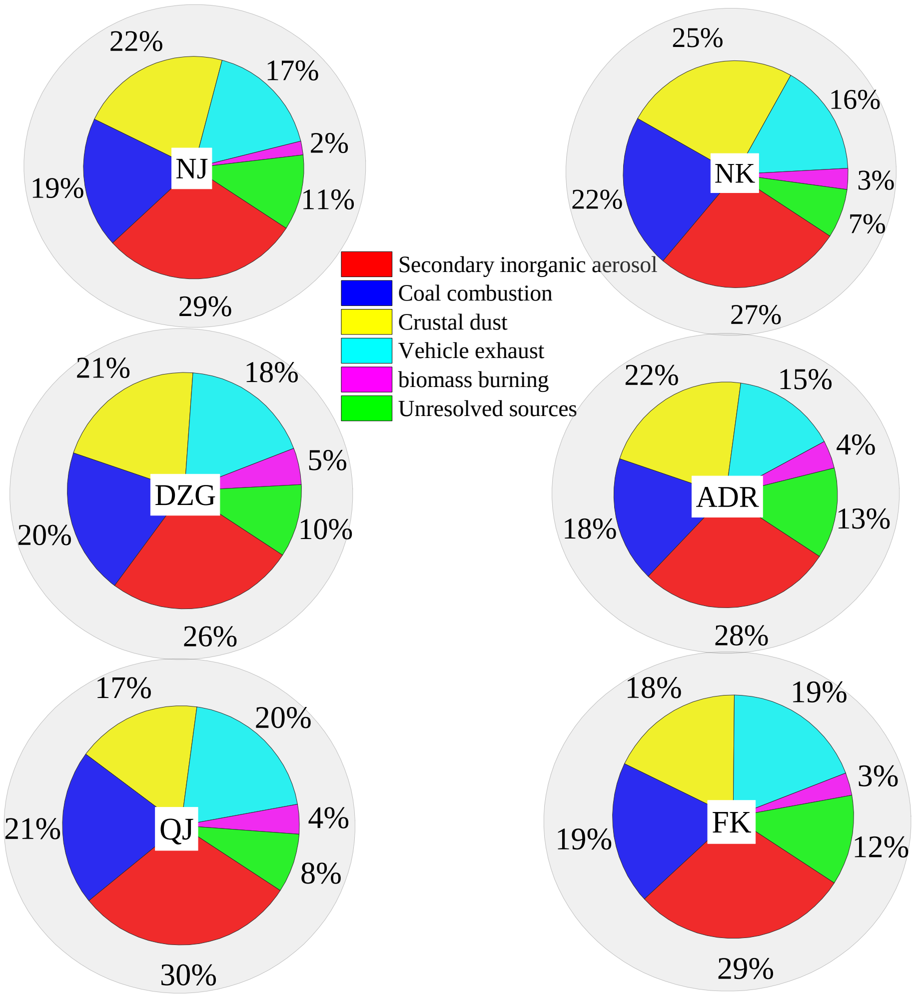

Fig. S8 The results of source apportionment for PM_{10} at different sampling sites during the heating period. NJ: Nanjing Road, NK: Nankou Road, DZG: Dazhigu Road, ADR: Advancing Road, QJ: Qinjian Road, FK: Fukang Road.

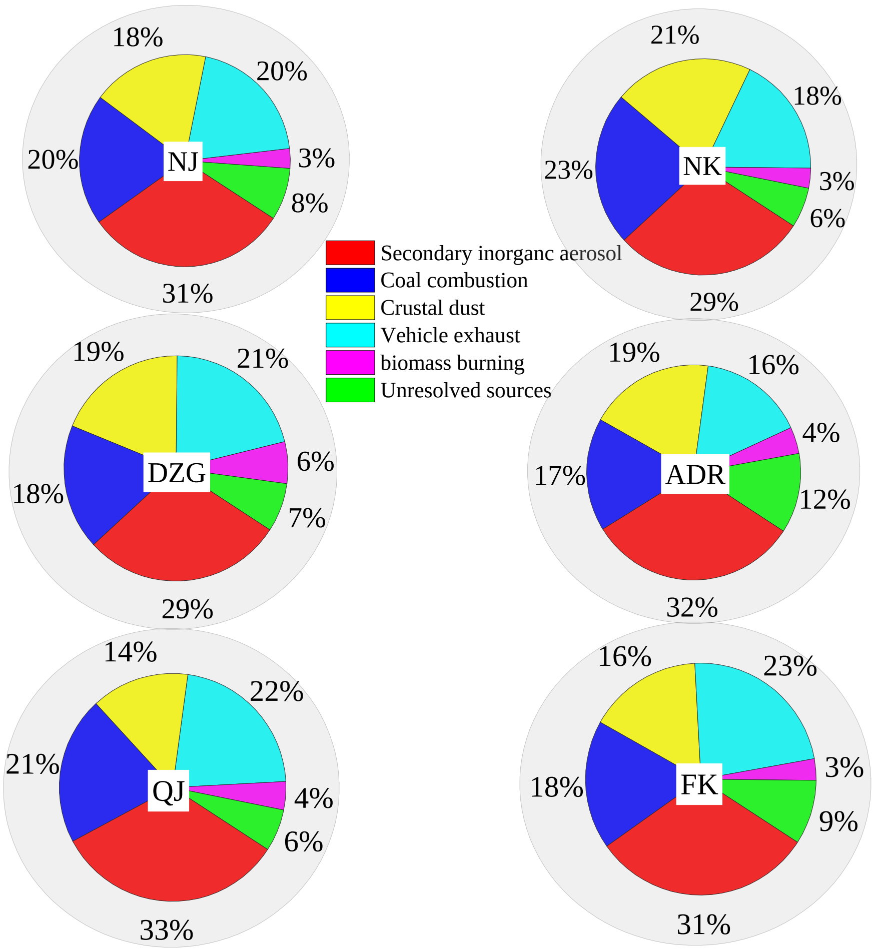

Fig. S9 The results of source apportionment for $PM_{2.5}$ at different sampling sites during the heating period. NJ: Nanjing Road, NK: Nankou Road, DZG: Dazhigu Road, ADR: Advancing Road, QJ: Qinjian Road, FK: Fukang Road.

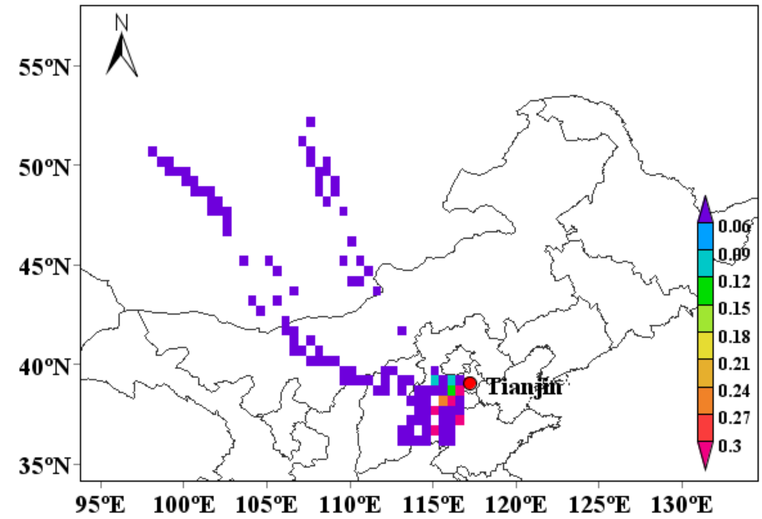

(1) PM_{10}

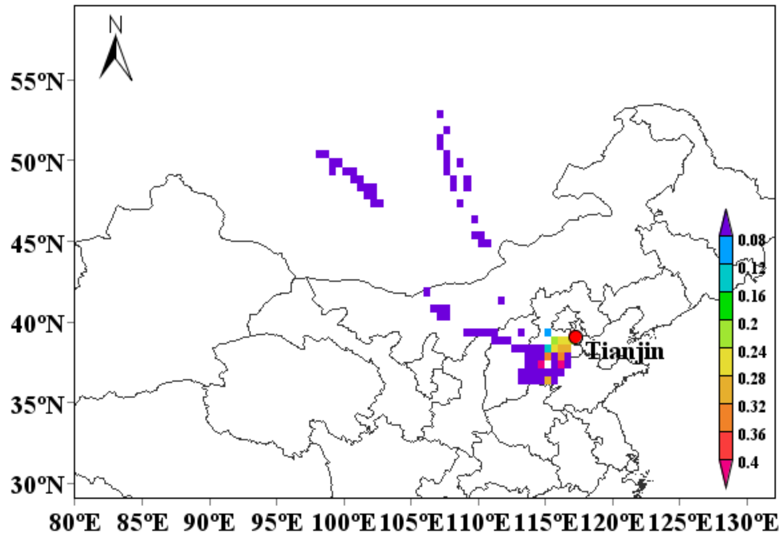

(2) $PM_{2.5}$

Fig. S10 The WPSCF maps for PM_{10} and $PM_{2.5}$ at Tian'jin. The red areas represent mainly potential source areas of PM_{10} and $PM_{2.5}$ concentrations.

Table S1 Descriptions of PM_{10} and $PM_{2.5}$ sampling sites in Tian'jin.

Sampling Sites	Latitude and Longitude	Descriptions
NJ	39.12º N;117.18º E	Educational, scenery and residential area
NK	39.17º N;117.19º E	Industrial and traffic area
DZG	39.11º N;117.24º E	Residential and commercial area
ADR	39.09º N;117.20º E	Residential, commercial and scenery area
QJ	39.17º N; 117.16º E	Traffic and residential area
FK	39.10º N;117.15º E	Educational, traffic and scenery area

NJ: Nanjing Road, NK: Nankou Road, DZG: Dazhigu Road, ADR: Advancing Road, QJ: Qinjian Road, FK: Fukang Road.

Table S2 The concentrations of gaseous pollutants (SO_2, NO_2, CO and O_3), and SOR, NOR at different sites in Tian'jin during the heating period.

Site	Index	SO_2 μg m^{-3}	NO_2 μg m^{-3}	CO mg m^{-3}	O_3 μg m^{-3}	SOR	NOR
NJ	Mean	34	55	1.3	**43**	0.15(PM_{10}) 0.10($PM_{2.5}$)	0.13(PM_{10}) 0.10($PM_{2.5}$)
	Maximum	69	93	2.3	66	0.23(PM_{10}) 0.18($PM_{2.5}$)	0.33(PM_{10}) 0.28($PM_{2.5}$)
	Minmum	14	22	0.7	28	0.09 (PM_{10}) 0.05($PM_{2.5}$)	0.04(PM_{10}) 0.02($PM_{2.5}$)
NK	Mean	39	51	**1.4**	23	0.14(PM_{10}) 0.11($PM_{2.5}$)	0.16(PM_{10}) 0.11($PM_{2.5}$)
	Maximum	63	82	2.1	34	0.31(PM_{10}) 0.19($PM_{2.5}$)	0.45(PM_{10}) 0.33($PM_{2.5}$)
	Minmum	25	26	1.0	17	0.07(PM_{10}) 0.06($PM_{2.5}$)	0.04(PM_{10}) 0.03($PM_{2.5}$)
DZG	Mean	33	50	1.0	40	0.14(PM_{10}) 0.14($PM_{2.5}$)	0.13(PM_{10}) 0.14($PM_{2.5}$)
	Maximum	61	83	2.0	58	0.24(PM_{10}) 0.26($PM_{2.5}$)	0.36(PM_{10}) 0.40($PM_{2.5}$)
	Minmum	16	21	0.4	26	0.08 (PM_{10}) 0.06($PM_{2.5}$)	0.04(PM_{10}) 0.03($PM_{2.5}$)
ADR	Mean	**46**	**58**	1.3	25	0.12(PM_{10}) 0.05($PM_{2.5}$)	0.08(PM_{10}) 0.04($PM_{2.5}$)
	Maximum	77	84	2.3	35	0.14(PM_{10}) 0.06($PM_{2.5}$)	0.11(PM_{10}) 0.06($PM_{2.5}$)
	Minmum	26	32	0.6	16	0.09 (PM_{10}) 0.03($PM_{2.5}$)	0.06(PM_{10}) 0.02($PM_{2.5}$)
QJ	Mean	25	54	1.1	39	0.22(PM_{10}) 0.20($PM_{2.5}$)	0.16(PM_{10}) 0.16($PM_{2.5}$)
	Maximum	48	99	2.2	60	0.32(PM_{10}) 0.33($PM_{2.5}$)	0.37(PM_{10}) 0.38($PM_{2.5}$)
	Minmum	10	20	0.5	27	0.13(PM_{10}) 0.09($PM_{2.5}$)	0.04(PM_{10}) 0.05($PM_{2.5}$)
FK	Mean	27	44	1.3	34	0.19(PM_{10}) 0.16($PM_{2.5}$)	0.16 (PM_{10}) 0.14($PM_{2.5}$)
	Maximum	54	75	2.2	52	0.29(PM_{10}) 0.25($PM_{2.5}$)	0.42(PM_{10}) 0.37($PM_{2.5}$)
	Minmum	8	17	0.7	23	0.13(PM_{10}) 0.11($PM_{2.5}$)	0.04(PM_{10}) 0.04($PM_{2.5}$)
TJ	Mean	34	52	1.2	34	0.17(PM_{10}) 0.13($PM_{2.5}$)	0.14 (PM_{10}) 0.11($PM_{2.5}$)
	Maximum	77	99	2.3	66	0.32(PM_{10}) 0.33($PM_{2.5}$)	0.45(PM_{10}) 0.40($PM_{2.5}$)
	Minmum	8	17	0.4	15.8	0.07(PM_{10}) 0.03($PM_{2.5}$)	0.04(PM_{10}) 0.02($PM_{2.5}$)

TJ represents the whole Tian'jin area. SOR and NOR represent sulfur and nitrogen oxidized ratios (the molar ratios of $[SO_4^{2-}]$ to $[SO_4^{2-} + SO_2]$, $[NO_3^-]$ to $[NO_3^- + NO_2]$, respectively).

Table S3 The method detection limits of chemical elements, the water-soluble inorganic ions, and carbonaceous species in this study.

Chemical species	Instruments	Units	Method Detection Limits
Al	Inductively Coupled Plasma-Atomic Emission Spectrometry	mg/L	0.0476
As	Inductively Coupled Plasma-Atomic Emission Spectrometry	mg/L	0.0064
Ca	Inductively Coupled Plasma-Atomic Emission Spectrometry	mg/L	0.2605
Cd	Inductively Coupled Plasma-Atomic Emission Spectrometry	mg/L	0.0003
Cr	Inductively Coupled Plasma-Atomic Emission Spectrometry	mg/L	0.0007
Cu	Inductively Coupled Plasma-Atomic Emission Spectrometry	mg/L	0.0073
Fe	Inductively Coupled Plasma-Atomic Emission Spectrometry	mg/L	0.0416
K	Inductively Coupled Plasma-Atomic Emission Spectrometry	mg/L	0.0191
Mg	Inductively Coupled Plasma-Atomic Emission Spectrometry	mg/L	0.0126
Mn	Inductively Coupled Plasma-Atomic Emission Spectrometry	mg/L	0.0004
Na	Inductively Coupled Plasma-Atomic Emission Spectrometry	mg/L	0.0210
Ni	Inductively Coupled Plasma-Atomic Emission Spectrometry	mg/L	0.0033
Pb	Inductively Coupled Plasma-Atomic Emission Spectrometry	mg/L	0.0044
Si	Inductively Coupled Plasma-Atomic Emission Spectrometry	mg/L	0.0304
V	Inductively Coupled Plasma-Atomic Emission Spectrometry	mg/L	0.0008
Zn	Inductively Coupled Plasma-Atomic Emission Spectrometry	mg/L	0.0060
Ti	Inductively Coupled Plasma-Atomic Emission Spectrometry	mg/L	0.0002
Na^+	Ion Chromatography	mg/L	0.008
Mg^{2+}	Ion Chromatography	mg/L	0.008
NH_4^+	Ion Chromatography	mg/L	0.031
NO_3^-	Ion Chromatography	mg/L	0.015
K^+	Ion Chromatography	mg/L	0.006
Ca^{2+}	Ion Chromatography	mg/L	0.033
Cl^-	Ion Chromatography	mg/L	0.014

SO_4^{2-}	Ion Chromatography	mg/L	0.043
OC	Desert Research Institute Model 2001 Thermal/optical Carbon Analyser	μg C/cm^2	0.82
EC	Desert Research Institute Model 2002 Thermal/optical Carbon Analyser	μg C/cm^2	0.20

The detection limits of chemical elements were determined based on the polypropylene membrane with 90 mm diameter, those of water-soluble inorganic ions and carbonaceous species were determined based on the quartz filter membrane with 90 mm diameter.

Table S4 The concentrations of PM_{10} and $PM_{2.5}$ in different cities around the world.

City	Sampling Period	Types	Season	Concentration (μg m^{-3})	References
Tian'jin	2016	PM_{10}	winter	98	This study
Bei'jing	2014-2015	PM_{10}	winter	114.9	Li et al., 2017
Zheng'zhou	2014-2015	PM_{10}	winter	263	Wang et al., 2017
Bao'shan Shang'hai	2009-2010	PM_{10}	winter	207.48	Wang et al., 2013
Hai'kou	2011-2012	PM_{10}	winter	77.23	Fang et al., 2017
Chong'qing	2012-2013	PM_{10}	annual mean	103.9	Chen et al., 2017
Southern Italy	2013-2014	PM_{10}	annual mean	29.5	Cesari et al., 2018
Bogota, Colombia	2015-2016	PM_{10}	dry season	34.6	Ramírez et al., 2018
Bogota, Colombia	2015-2016	PM_{10}	rainy season	41.4	Ramírez et al., 2018
Tian'jin	2016	$PM_{2.5}$	winter	71	This study
Bei'jing	2000-2010	$PM_{2.5}$	winter	140.1	Lv et al., 2016
Xin'xiang	2015	$PM_{2.5}$	winter	111	Feng et al., 2016
Lang'fang	2014	$PM_{2.5}$	annual mean	150	Gao et al., 2018

Bao'ding	2014	$PM_{2.5}$	annual mean	180	Gao et al., 2018
Tai'yuan	2009-2010	$PM_{2.5}$	winter	257.29	He et al., 2017
Zheng'zhou	2014-2015	$PM_{2.5}$	winter	179	Wang et al., 2017
Guang'zhou	2012-2013	$PM_{2.5}$	winter	40.8	Lai et al., 2016
Shang'hai	2013-2014	$PM_{2.5}$	slight haze	146.9	Qiao et al., 2016
Hai'kou	2011-2012	$PM_{2.5}$	winter	48.14	Fang et al., 2017
Seoul	2014	$PM_{2.5}$	annual mean	31	Park et al., 2018
Baengnyeong	2015-2016	$PM_{2.5}$	annual mean	30	Park et al., 2018
Southern Italy	2013-2014	$PM_{2.5}$	annual mean	18.7	Cesari et al., 2018

Reference

Cesari, D., Benedetto De, G. E., Bonasoni, P., Busetto, M., Dinoi, A., Merico, E., Chirizzi, D., Cristofanelli, P., Donateo, A., Grasso, F. M., Marinoni, A., Pennetta, A. and Daniele, C. (2018). Seasonal variability of $PM_{2.5}$ and PM_{10} composition and sources in an urban background site in southern Italy. *Sci. Total Environ.* 612: 202–213.

Chen, Y., Xie, X.D., Luo, B. and Zhai, C.Z. (2017). Particulate pollution in urban Chongqing of southwest China: Historical trends of variation, chemical characteristics and source apportionment. *Sci. Total Environ.* 584–585: 523–534.

Fang, X., Bi, X., Xu, H., Wu, J., Zhang, Y. and Feng, Y. (2017). Source apportionment of ambient PM_{10}, and $PM_{2.5}$ in Haikou, China. *Atmos. Res.* 190: 1–9.

Feng, J., Yu, H., Su, X., Liu, S., Li, Y., Pan, Y. and Sun, J.H. (2016). Chemical composition and source apportionment of $PM_{2.5}$ during Chinese Spring Festival at Xinxiang, a heavily polluted city in North China: Fireworks and health risks. *Atmos. Res.* 182: 176–188.

Gao, J., Wang, K., Wang, Y., Liu, S., Zhu, C., Hao, J. and Liu, H. (2018). Temporal-spatial characteristics and source apportionment of $PM_{2.5}$ as well as its associated chemical species in the Beijing-Tianjin-Hebei region of China. *Environ. Pollut.* 233: 714–724.

He, Q.S., Yan, Y.L., Guo, L.L., Zhang, Y.L., Zhang, G.X. and Wang, X.M. (2017). Characterization and source analysis of water-soluble inorganic ionic species in $PM_{2.5}$ in Taiyuan city, China. *Atmos. Res.* 184: 48–55.

Lai, S.C., Zhao, Y., Ding, A.J., Zhang, Y.Y., Song, T.L., Zheng, J.Y., Ho, K.F., Lee, S.C. and Zhong, L.J. (2016). Characterization of $PM_{2.5}$, and the major chemical components during a 1-year campaign in rural Guangzhou, Southern China. *Atmos. Res.* 167: 208–215.

Li, D.P., Liu, J., Zhang, J.G., Zhang, J.S., Gui, H.Q., Du, P., Yu, T.Z., Wang, J., Lu, Y.H., Liu, W.Q. and Cheng, Y. (2017). Identification of long-range transport pathways and potential sources of $PM_{2.5}$ and PM_{10} in Beijing from 2014 to 2015. *J. Environ. Sci.* 56: 214–229.

Lv, B., Zhang B. and Bai Y. (2016). A systematic analysis of $PM_{2.5}$ in Beijing and its sources from 2000 to 2012. *Atmos. Environ.* 124: 98–108.

Park, Y.M., Park, K.S., Kim, H., Yu, S. M., Noh, S., Kim, M.S., Kim, J.Y., Ahn, J.Y., Lee, M.D., Seok, K.S. and Kim, Y.H. (2018). Characterizing isotopic compositions of TC-C, NO_3^--N, and NH_4^+-N in $PM_{2.5}$ in South Korea: Impact of China's winter heating. *Environ. Pollut.* 233: 735–744.

Qiao, T., Zhao, M.F., Xiu, G.L. and Yu, J.Z. (2016). Simultaneous monitoring and compositions analysis of PM_1 and $PM_{2.5}$ in Shanghai: Implications for characterization of haze pollution and source apportionment. *Sci. Total Environ.* 557–558: 386–394.

Ramírez, O., Sánchez, A.D.L.C., Amato, F., Catacolí, R.A., Rojas, N.Y. and De, J.L.R. (2018). Chemical composition and source apportionment of PM_{10}, at an urban background site in a high–altitude Latin American megacity (Bogota, Colombia). *Environ. Pollut.* 233: 142–155.

Wang, Q., Jiang, N., Yin, S.S, Li, X., Yu, F., Guo, Y. and Zhang, R.Q. (2017). Carbonaceous species in $PM_{2.5}$ and PM_{10} in urban area of Zhengzhou in China: Seasonal variations and source apportionment. *Atmos. Res.* 191: 1–11.

Wang, J., Hu, Z.M., Chen, Y.Y, Chen, Z.L. and Xu, S.Y. (2013). Contamination characteristics and possible sources of PM_{10} and $PM_{2.5}$ in different functional areas of Shanghai, China. *Atmos. Environ.* 68: 221–229.

Table S5 Pearson's correlations (*r*) between the water-soluble ions in PM_{10} and $PM_{2.5}$ in Tian'jin during the heating period.

PM_{10}								
	Cl^-	NO_3^-	SO_4^{2-}	Na^+	NH_4^+	K^+	Mg^{2+}	Ca^{2+}
Cl^-	1	0.54**	0.43**	0.14	0.42**	0.56**	0.02	-0.23
NO_3^-		1	0.73**	-0.35*	0.71**	0.20	-0.51**	-0.14
SO_4^{2-}			1	-0.37**	0.64**	0.24	-0.18	0.02
Na^+				1	-0.44**	0	0.50**	0.32*
NH_4^+					1	0.16	-0.51**	-0.32*
K^+						1	0.30*	-0.31*
Mg^{2+}							1	0.71**
Ca^{2+}								1
$PM_{2.5}$								
	Cl^-	NO_3^-	SO_4^{2-}	Na^+	NH_4^+	K^+	Mg^{2+}	Ca^{2+}
Cl^-	1	0.51**	0.43**	0.09	0.37**	0.81**	-0.07	-0.40**
NO_3^-		1	0.82**	-0.43**	0.81**	0.40**	-0.63**	-0.69**
SO_4^{2-}			1	-0.23	0.77**	0.44**	-0.39**	-0.60**
Na^+				1	-0.40**	0.16	0.57**	0.56**
NH_4^+					1	0.21	-0.65**	-0.72**
K^+						1	0.13	-0.36*
Mg^{2+}							1	0.54*
Ca^{2+}								1

* represent extremely significant correlation ($p < 0.05$)

** represent extremely significant correlation ($p < 0.01$)

Table S6 The ratios of OC/EC and levels of secondary organic carbon (SOC) estimated from minimum OC/EC ratios.

Sites	OC/EC		$(OC/EC)_{min}$		SOC Concentration ($\mu g\ m^{-3}$)		Percentage (SOC/OC, %)	
	PM_{10}	$PM_{2.5}$	PM_{10}	$PM_{2.5}$	PM_{10}	$PM_{2.5}$	PM_{10}	$PM_{2.5}$
NJ	3.3	3.1	2.8	2.4	1.9	1.9	14.0	23.7
NK	3.2	2.8	1.8	2.3	3.8	3.8	36.9	27.4
DZG	3.3	3.1	2.7	2.4	1.6	1.9	16.6	20.4
ADR	2.9	3.4	2.1	2.8	4.0	2.3	23.7	18.2
QJ	3.1	3.3	2.6	2.4	2.4	0.5	17.9	11.5
FK	2.8	3.1	2.2	2.2	2.1	2.4	22.9	26.3
TJ	3.1	3.2	1.8	2.2	4.8	2.8	39.8	28.0

NJ: Nanjing Road, NK: Nankou Road, DZG: Dazhigu Road, ADR: Advancing Road, QJ: Qinjian Road, FK: Fukang Road. TJ: Tianjin city.

Table S7 Linear regression parameters of OC and EC based on different percentiles of OC/EC ratios in the whole Tian'jin city. The regression of OC and EC data below 10th percentile of OC/EC ratios shows the best solution to calculate the primary OC/EC ratio.

Percentiles of OC/EC ratios	OC/EC		r^2		Slope	
	$PM_{2.5}$	PM_{10}	$PM_{2.5}$	PM_{10}	$PM_{2.5}$	PM_{10}
10th	**2.2**	**1.8**	**0.99**	**0.96**	**0.41**	**0.43**
20th	2.5	2.3	0.99	0.95	0.37	0.42
30th	2.6	2.5	0.98	0.94	0.36	0.45
40th	2.6	2.6	0.97	0.91	0.35	0.38
50th	2.7	2.7	0.97	0.9	0.35	0.33
60th	2.8	2.7	0.98	0.91	0.35	0.32
70th	2.9	2.8	0.96	0.90	0.34	0.33
80th	2.9	2.9	0.94	0.89	0.33	0.32

Table S8 Linear regression parameters of OC and EC based on different percentiles of OC/EC ratios at Nanjing road (NJ) site. The regression of OC and EC data below 10th percentile of OC/EC ratios shows the best solution to calculate the primary OC/EC ratio.

Percentiles of OC/EC ratios	OC/EC		r^2		Slope	
	$PM_{2.5}$	PM_{10}	$PM_{2.5}$	PM_{10}	$PM_{2.5}$	PM_{10}
10th	**2.4**	**2.8**	**0.99**	**0.99**	**0.38**	**0.36**
20th	2.5	2.9	0.98	0.98	0.36	0.36
30th	2.6	2.9	0.99	0.98	0.36	0.34
40th	2.6	3.0	0.97	0.97	0.35	0.33
50th	2.7	3.0	0.97	0.98	0.35	0.32
60th	2.8	3.1	0.98	0.97	0.33	0.31
70th	2.8	3.1	0.98	0.98	0.34	0.32
80th	2.9	3.2	0.97	0.98	0.31	0.31

Table S9 Linear regression parameters of OC and EC based on different percentiles of OC/EC ratios at Nankou road (NK) site. The regression of OC and EC data below 10th percentile of OC/EC ratios shows the best solution to calculate the primary OC/EC ratio.

Percentiles of OC/EC ratios	OC/EC		r^2		Slope	
	$PM_{2.5}$	PM_{10}	$PM_{2.5}$	PM_{10}	$PM_{2.5}$	PM_{10}
10th	**2.3**	**1.8**	**0.99**	**0.98**	**0.46**	**0.42**
20th	2.4	1.9	0.98	0.91	0.42	0.42
30th	2.4	2.0	0.98	0.87	0.43	0.41
40th	2.5	2.2	0.97	0.82	0.42	0.41
50th	2.5	2.3	0.97	0.73	0.41	0.4
60th	2.6	2.4	0.93	0.69	0.41	0.39
70th	2.7	2.6	0.94	0.56	0.39	0.39
80th	2.8	2.8	0.93	0.48	0.39	0.37

Table S10 Linear regression parameters of OC and EC based on different percentiles of OC/EC ratios at Dazhigu road (DZG) site. The regression of OC and EC data below 10th percentile of OC/EC ratios shows the best solution to calculate the primary OC/EC ratio.

Percentiles of OC/EC ratios	OC/EC		r^2		Slope	
	$PM_{2.5}$	PM_{10}	$PM_{2.5}$	PM_{10}	$PM_{2.5}$	PM_{10}
10th	**2.4**	**2.7**	**1.00**	**1.00**	**0.38**	**0.35**
20th	2.5	2.9	0.99	0.99	0.37	0.33
30th	2.6	2.9	0.98	0.98	0.37	0.33
40th	2.6	3.0	0.97	0.97	0.36	0.32
50th	2.7	3.1	0.95	0.98	0.35	0.31
60th	2.8	3.2	0.95	0.96	0.32	0.31
70th	2.8	3.3	0.96	0.97	0.32	0.30
80th	2.9	3.3	0.95	0.96	0.31	0.29

Table S11 Linear regression parameters of OC and EC based on different percentiles of OC/EC ratios at Advancing road (ADR) site. The regression of OC and EC data below 10th percentile of OC/EC ratios shows the best solution to calculate the primary OC/EC ratio.

Percentiles of OC/EC ratios	OC/EC		r^2		Slope	
	$PM_{2.5}$	PM_{10}	$PM_{2.5}$	PM_{10}	$PM_{2.5}$	PM_{10}
10th	**2.8**	**2.1**	**0.99**	**0.99**	**0.38**	**0.46**
20th	2.8	2.2	0.98	0.98	0.36	0.45
30th	2.9	2.4	0.97	0.98	0.36	0.44
40th	3.0	2.4	0.97	0.97	0.35	0.42
50th	3.1	2.5	0.98	0.95	0.34	0.41
60th	3.1	2.7	0.97	0.89	0.32	0.41
70th	3.2	2.8	0.96	0.85	0.31	0.4
80th	3.2	2.9	0.97	0.84	0.31	0.39

Table S12 Linear regression parameters of OC and EC based on different percentiles of OC/EC ratios at Qinjian road (QJ) site. The regression of OC and EC data below 10th percentile of OC/EC ratios shows the best solution to calculate the primary OC/EC ratio.

Percentiles of OC/EC ratios	OC/EC		r^2		Slope	
	$PM_{2.5}$	PM_{10}	$PM_{2.5}$	PM_{10}	$PM_{2.5}$	PM_{10}
10th	**2.4**	**2.6**	**0.98**	**1.00**	**0.43**	**0.36**
20th	2.5	2.7	0.97	0.99	0.42	0.35
30th	2.6	2.7	0.97	0.97	0.41	0.35
40th	2.8	2.8	0.96	0.97	0.39	0.34
50th	2.9	2.8	0.96	0.98	0.39	0.34
60th	3.0	2.9	0.97	0.97	0.38	0.33
70th	3.1	3.0	0.96	0.96	0.37	0.31
80th	3.1	3.1	0.97	0.95	0.35	0.31

Table S13 Linear regression parameters of OC and EC based on different percentiles of OC/EC ratios at Fukang road (FK) site. The regression of OC and EC data below 10th percentile of OC/EC ratios shows the best solution to calculate the primary OC/EC ratio.

Percentiles of OC/EC ratios	OC/EC		r^2		Slope	
	$PM_{2.5}$	PM_{10}	$PM_{2.5}$	PM_{10}	$PM_{2.5}$	PM_{10}
10th	**2.2**	**2.2**	**0.98**	**0.99**	**0.39**	**0.49**
20th	2.3	2.3	0.98	0.99	0.38	0.48
30th	2.4	2.4	0.97	0.98	0.37	0.47
40th	2.6	2.5	0.96	0.97	0.38	0.46
50th	2.7	2.5	0.96	0.97	0.35	0.45
60th	2.8	2.6	0.95	0.96	0.34	0.44
70th	2.9	2.6	0.94	0.95	0.33	0.43
80th	3.0	2.7	0.93	0.95	0.34	0.39

Table S14 Summary of PMF and EE diagnostics by run for PM_{10} data in Tian'jin during the heating period.

Diagnostic	2 factors	3factors	4 factors	5 factors	6 factors	7 factors	8 factors
$Q_{expected}$	986	915	844	773	702	631	560
Q_{true}	10437	8499	6641	4865	3395	2450	1810
Q_{robust}	7986	5860	4467	3442	2922	2302	1838
$Q_{robust}/Q_{expected}$	8.1	6.4	5.3	4.5	4.2	3.6	3.3
DISP %dQ	<0.1%	<0.1%	<0.1%	<0.1%	<0.1%	<0.1%	<0.1%
DISP swaps	0	0	0	0	0	0	0
Factors with BS mapping <100%						6^{th} F:95%	

F represents Factor

Table S15 Summary of PMF and EE diagnostics by run for $PM_{2.5}$ data in Tian'jin during the heating period.

Diagnostic	2 factors	3factors	4 factors	5 factors	6 factors	7 factors	8 factors
$Q_{expected}$	920	852	784	716	648	580	512
Q_{true}	13799	10041	7167	4822	3530	2575	1860
Q_{robust}	8258	6119	4789	3650	2940	2287	1748
$Q_{robust}/Q_{expected}$	9.0	7.2	6.1	5.1	4.5	3.9	3.4
DISP %dQ	<0.1%	<0.1%	<0.1%	<0.1%	<0.1%	<0.1%	<0.1%
DISP swaps	0	0	0	0	0	0	0
Factors with BS mapping <100%		2^{nd} F:90%			6^{th} F:95%	2^{nd}F:90%	7^{th} F: 95%

F represents Factor